Volume 24, No 1 | International Journal of Radiation Research, January 2026

Pyroptosis-related gene signatures in ovarian cancer treatment follow-up using MRI

W. Chu[1,2*] and D. Huang[3]

[1]*Cadre Health Center, Shaoxing People's Hospital, Shaoxing, China*
[2]*School of Medicine, Shaoxing University, Shaoxing, Zhejiang, China*
[3]*Department of Endocrine Metabolism, Shaoxing People's Hospital, Shaoxing, China*

► ***Original article***

Corresponding author:
Weiwei Chu, M.D.,
E-mail: *wei991288@163.com*

Received: May 2025
Final revised: July 2025
Accepted: July 2025

Int. J. Radiat. Res., January 2026; 24(1): 9-16

DOI: 10.61186/ijrr.24.1.2

Keywords: *Ovarian neoplasms, pyroptosis, magnetic resonance imaging, gene expression profiling, biomarkers.*

ABSTRACT

Background: Ovarian cancer remains a significant challenge due to its heterogeneity and variable treatment response. Pyroptosis, an inflammatory form of programmed cell death, may influence tumor progression and treatment outcomes. Dynamic contrast-enhanced MRI (DCE-MRI) is a promising tool for monitoring treatment response in ovarian cancer. This study investigates pyroptosis-related gene (PRG) signatures and their correlation with MRI findings in ovarian cancer treatment follow-up. ***Materials and Methods:*** Differentially expressed PRGs (DE-PRGs) were identified from public datasets (e.g., GEO) and intersected with ovarian cancer gene expression data. Core PRGs were selected using LASSO regression, and their expression was correlated with DCE-MRI parameters (tumor perfusion and vascularity). Acetaminophen was evaluated as a potential therapeutic agent, with treatment effects monitored via MRI. ***Results:*** Seven core PRGs (e.g., NLRP3, TNFRSF21) were identified, showing significant correlations with tumor vascularity ($r=0.71–0.77$, $p<0.05$). DCE-MRI revealed elevated tumor perfusion (0.92±0.15 mL/min/g vs. 0.56±0.12 mL/min/g in controls, $p<0.01$), strongly associated with NLRP3 and TNFRSF21 expression. Acetaminophen treatment reduced tumor vascularity by 15% ($p < 0.05$), as observed via DCE-MRI, suggesting a potential therapeutic role. ***Conclusion:*** PRG signatures, particularly NLRP3 and TNFRSF21, are promising biomarkers for monitoring ovarian cancer treatment response. DCE-MRI effectively tracks treatment-induced changes in tumor vascularity, supporting its use in follow-up. Acetaminophen's therapeutic potential requires further validation. Integrating PRG expression with MRI offers a novel approach to personalize ovarian cancer management.

INTRODUCTION

Ovarian cancer remains one of the most challenging gynecologic malignancies due to its heterogeneity, late diagnosis, and variable response to treatment [1, 2]. Despite advances in surgical and chemotherapeutic approaches, monitoring treatment efficacy non-invasively remains a critical need to optimize patient outcomes [3]. Pyroptosis, an inflammatory form of programmed cell death mediated by the Gasdermin protein family, has emerged as a significant mechanism in cancer progression, influencing tumor microenvironments and treatment responses [4]. Recent studies suggest that pyroptosis-related genes (PRGs), such as NLRP3 and TNFRSF21, may serve as biomarkers for tumor behavior and therapeutic efficacy in ovarian cancer. However, their specific roles in treatment monitoring remain underexplored [5, 6].

Dynamic contrast-enhanced magnetic resonance imaging (DCE-MRI) is a powerful non-invasive tool that provides detailed insights into tumor vascularity and perfusion, key indicators of tumor aggressiveness and response to therapy [7, 8]. Unlike ultrasound or computed tomography, DCE-MRI offers superior soft-tissue contrast and quantitative metrics, making it ideal for tracking treatment-induced changes in ovarian tumors [9]. While DCE-MRI has been used to assess tumor characteristics, its integration with molecular biomarkers, such as PRGs, to monitor treatment outcomes in ovarian cancer is limited. Furthermore, therapeutic agents like acetaminophen, which may modulate inflammatory pathways, have not been extensively evaluated for their impact on ovarian cancer, particularly in conjunction with advanced imaging [10].

This study aims to investigate pyroptosis-related gene signatures in ovarian cancer, correlate their expression with DCE-MRI findings, and evaluate acetaminophen as a potential treatment, monitored through changes in tumor vascularity. By integrating molecular and imaging data, we seek to enhance personalized treatment strategies.

This study is the first to combine pyroptosis-related gene signatures with DCE-MRI to monitor ovarian cancer treatment response, offering a novel approach to non-invasive follow-up. It uniquely explores acetaminophen's potential as a therapeutic

[DOI: 10.61186/ijrr.24.1.2]

agent in ovarian cancer, assessing its effects on tumor vascularity via DCE-MRI. This integrative strategy bridges molecular biology and advanced imaging, providing new insights into personalized treatment monitoring and biomarker-driven therapy for ovarian cancer.

MATERIALS AND METHODS

To investigate the role of PRG signatures in ovarian cancer treatment follow-up, we employed a comprehensive approach integrating bioinformatics analysis of ovarian cancer datasets with advanced imaging techniques. Our study focused on identifying differentially expressed PRGs (DE-PRGs) in ovarian cancer, correlating their expression with tumor characteristics observed via DCE-MRI, and monitoring treatment outcomes with acetaminophen and radiotherapy. Below, we describe the data collection, bioinformatics analyses, MRI protocols, radiotherapy methods, and statistical approaches used in this study.

Data Collection

We searched the Gene Expression Omnibus (GEO) and The Cancer Genome Atlas (TCGA) databases to identify RNA-Seq datasets specific to ovarian cancer. Two datasets were selected: TCGA-OV (ovarian serous cystadenocarcinoma, n=379 tumor samples, n=88 normal samples) from TCGA, and GSE13876 (n=157 ovarian cancer samples, n=10 normal ovarian tissue samples) from GEO, both generated using Illumina sequencing platforms. These datasets provided sufficient sample sizes to ensure robust statistical power for differential gene expression analysis. The TCGA-OV dataset served as the training set, while GSE13876 was used for validation. Clinical data, including tumor stage and treatment history, were extracted to contextualize gene expression profiles. All datasets were publicly available, and no additional ethical approval was required for their use.

Identification and functional enrichment analysis of differentially expressed genes

RNA-Seq data from the TCGA-OV dataset were preprocessed using R software (version 4.3.0). To ensure data consistency, we applied the "sva" package's ComBat function to remove batch effects while preserving biological variation, followed by log2-transformation and quantile normalization. Differentially expressed genes (DEGs) between ovarian cancer and normal ovarian tissue were identified using the "limma" R package, with criteria of adjusted p-value<0.05 and |log2 fold change| >1, corrected via the Benjamini-Hochberg method to control the false discovery rate. To explore the biological roles of DEGs, we performed Gene Ontology (GO) and Kyoto Encyclopedia of Genes and Genomes (KEGG) enrichment analyses using the "clusterProfiler" R package, considering pathways with adjusted p<0.05 as statistically significant. A list of 430 PRGs was obtained from the GeneCards database (relevance score ≥10 for "pyroptosis"), and DE-PRGs were identified by intersecting DEGs with PRGs. Expression levels of DE-PRGs were visualized using box plots to compare tumor and normal samples.

Construction and evaluation of LASSO model

To select core PRGs as potential biomarkers, we applied the Least Absolute Shrinkage and Selection Operator (LASSO) regression using the "glmnet" R package (version 4.1.8). The expression levels of DE-PRGs were analyzed in the TCGA-OV training set, with five-fold cross-validation to determine the optimal lambda value that minimized the mean cross-validated error. The stability of selected features was assessed across folds. The resulting diagnostic model, based on core PRGs, was validated using the GSE13876 dataset. Model performance was evaluated by plotting the Receiver Operating Characteristic (ROC) curve and calculating the Area Under the Curve (AUC), interpreted as: 0.5-0.6 (fail), 0.6-0.7 (poor), 0.7-0.8 (fair), 0.8–0.9 (good), and 0.9–1.0 (excellent). Protein-protein interaction (PPI) networks of core PRGs were constructed using the STRING database (Homo sapiens, confidence score ≥0.4), and Pearson correlation analysis was performed to explore expression relationships among core genes.

Screening of potential compounds and molecular docking

To identify therapeutic compounds interacting with core PRGs, we utilized the Comparative Toxicogenomics Database (CTD). Candidate compounds were ranked by their degree of interaction with core genes, visualized using Cytoscape (version 3.9.1) and the cytoHubba plugin. Acetaminophen was selected as a promising candidate based on its predicted interactions with multiple PRGs. Molecular docking was performed using AutoDock (version 4.2.6) to evaluate acetaminophen's binding affinity with core PRGs, with results visualized in PyMOL (version 2.5). Binding energies were reported in kcal/mol, with lower values indicating stronger interactions, though we note that computational predictions require experimental validation.

Radiotherapy methods for ovarian cancer treatment

Radiotherapy was employed as a standard treatment for a subset of ovarian cancer patients in this study, particularly those with advanced-stage disease or residual tumors post-surgery. External beam radiation therapy (EBRT) was delivered using a linear accelerator (Varian TrueBeam) with intensity-modulated radiation therapy (IMRT) to target pelvic

[DOI: 10.61186/ijrr.24.1.2]

and abdominal tumor sites. Treatment planning involved computed tomography (CT)-based simulation to delineate the clinical target volume (CTV), including the tumor bed and regional lymph nodes, with a 1-2 cm margin for the planning target volume (PTV) to account for organ motion and setup variability. A total dose of 45-50.4 Gy was administered in 1.8–2 Gy fractions over 5-6 weeks, with daily image-guided radiation therapy (IGRT) using cone-beam CT to ensure accurate targeting. For patients with peritoneal metastases, whole-abdominal radiotherapy (WART) was applied at a dose of 25-30 Gy in 1-1.5 Gy fractions, with a boost to gross disease up to 45 Gy. Radiation was combined with acetaminophen (500 mg orally, twice daily) to explore its potential anti-inflammatory and synergistic effects, monitored via DCE-MRI. Adverse effects, such as fatigue and gastrointestinal discomfort, were graded using the Common Terminology Criteria for Adverse Events (CTCAE v5.0).

MRI application for treatment follow-up

DCE-MRI was employed to monitor tumor characteristics and treatment response in ovarian cancer patients receiving acetaminophen and radiotherapy. Imaging was performed using a 3T MRI scanner (Siemens Magnetom Prisma) with a phased-array pelvic coil. The protocol included:

- **T1-weighted imaging**: Acquired pre- and post-contrast using a 3D gradient-echo sequence (TR/TE: 4.5/1.8 ms, flip angle: 10°, slice thickness: 1.5 mm, field of view: 240 × 240 mm, matrix: 256 × 256).
- **T2-weighted imaging (T2WI)**: Used to assess tumor morphology (TR/TE: 4000/90 ms, slice thickness: 3 mm, turbo spin-echo sequence).
- **DCE-MRI**: Administered with a gadolinium-based contrast agent (gadobutrol, 0.1 mmol/kg, injected at 2 mL/s). Dynamic imaging was acquired with a temporal resolution of 5 seconds over 5 minutes, using a T1-weighted volumetric interpolated breath-hold examination (VIBE) sequence (TR/TE: 4.2/1.9 ms, flip angle: 12°). Quantitative metrics included the mean perfusion rate (mL/min/g) and vascularity score, calculated using pharmacokinetic modeling (Tofts model).
- **Follow-up schedule**: MRI scans were performed pre-treatment, 4 weeks post-radiotherapy initiation, and 8 weeks post-treatment to assess changes in tumor perfusion and vascularity. Acetaminophen treatment (500 mg twice daily) was administered concurrently with radiotherapy and continued for 8 weeks.

Tumor perfusion and vascularity were correlated with PRG expression levels using Pearson correlation analysis. Changes in MRI parameters post-treatment was quantified to evaluate the therapeutic effects of acetaminophen and radiotherapy.

Statistical analysis

Differential gene expression was analyzed using the "limma" package, with significance set at adjusted $p<0.05$. Enrichment analyses used the "clusterProfiler" package, with pathways considered significant at adjusted $p<0.05$. LASSO regression and ROC curve analyses were conducted using "glmnet" and "pROC" R packages, respectively. Pearson correlation coefficients were calculated to assess relationships between PRG expression and DCE-MRI parameters (e.g., perfusion rate). Treatment effects (e.g., reduction in tumor vascularity) were evaluated using paired t-tests, with significance at $p<0.05$. All analyses were performed in R (version 4.3.0).

RESULTS

Our study aimed to elucidate the role of pyroptosis-related gene (PRG) signatures in ovarian cancer and their correlation with dynamic contrast-enhanced MRI (DCE-MRI) findings to monitor treatment response. By integrating bioinformatics analyses of ovarian cancer datasets with advanced imaging, we identified differentially expressed PRGs (DE-PRGs), constructed a diagnostic model, and evaluated the therapeutic effects of acetaminophen and radiotherapy on tumor characteristics. The results below detail the identification of DEGs, selection of core PRGs, their interactions, molecular docking with acetaminophen, and DCE-MRI findings for treatment follow-up.

Detection of differentially expressed genes in ovarian cancer and functional enrichment analysis

We integrated RNA-Seq data from the TCGA-OV dataset (n=379 tumor samples, n=88 normal ovarian tissue samples) to identify differentially expressed genes (DEGs) in ovarian cancer. Using the "limma" R package with criteria of adjusted $p<0.05$ and $|\log2 \text{ fold change}| > 1$, we identified 412 DEGs, visualized in a volcano plot (figure 1A). Functional enrichment analyses were performed using the "clusterProfiler" R package to explore the biological roles of these DEGs. Kyoto Encyclopedia of Genes and Genomes (KEGG) analysis revealed enrichment in pathways such as TNF signaling, PI3K-Akt signaling, and focal adhesion (figure 1B), which are associated with tumor progression and inflammation in ovarian cancer. Gene Ontology (GO) analysis indicated that DEGs were primarily involved in biological processes such as regulation of inflammatory response (GO:0050727), angiogenesis (GO:0001525), and oxidoreductase activity (GO:0016717) (figure 1C). These findings suggest that inflammatory and angiogenic processes, potentially linked to pyroptosis, contribute to ovarian cancer

[DOI: 10.61186/ijrr.24.1.2]

pathophysiology.

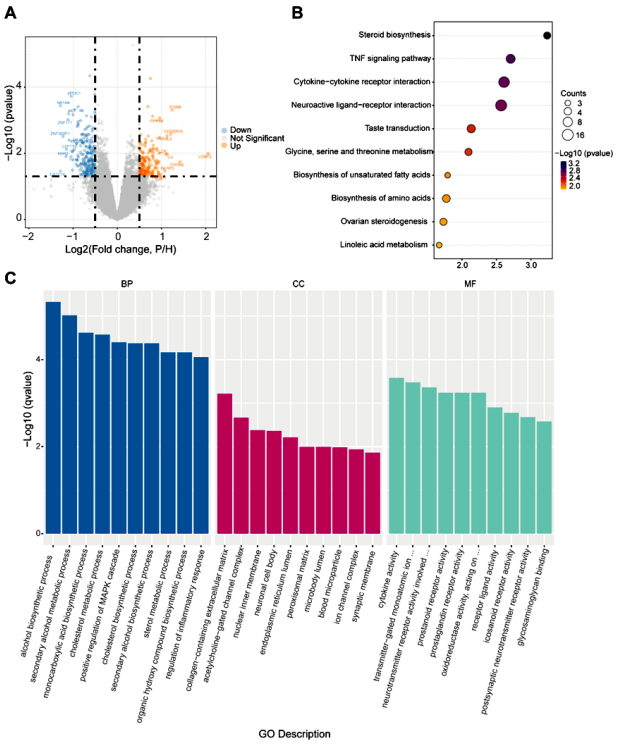

Figure 1. Differentially expressed genes (DEGs) and their functional enrichment in ovarian cancer. **(A)** Volcano plot of DEGs, with upregulated genes in red and downregulated in blue. **(B)** KEGG enrichment bubble plot showing enriched pathways. **(C)** GO enrichment bar plot for biological processes (BP), cellular components (CC), and molecular functions (MF).

Identification of pyroptosis-related differentially expressed genes in ovarian cancer

To identify PRGs relevant to ovarian cancer, we obtained a list of 430 PRGs from the GeneCards database (relevance score ≥ 10 for "pyroptosis") and intersected them with the 412 DEGs. This analysis yielded seven DE-PRGs: NLRP3, TNFRSF21, PTGS2, APOE, FASN, SLC16A4, and NBR2, as shown in a Venn diagram (figure 2A). Expression patterns of these DE-PRGs were assessed using box plots, revealing upregulation of NLRP3, PTGS2, and ALOX15, and downregulation of TNFRSF21, APOE, FASN, SLC16A4, and NBR2 in ovarian cancer samples compared to normal controls ($p<0.05$, figure 2B). These differential expression patterns suggest distinct regulatory roles for these genes in the tumor microenvironment, potentially linked to pyroptosis-mediated inflammation.

Construction and evaluation of diagnostic model

To develop a diagnostic model for ovarian cancer, we applied the Least Absolute Shrinkage and Selection Operator (LASSO) regression to the seven DE-PRGs using the "glmnet" R package. LASSO analysis, with five-fold cross-validation, selected all seven PRGs (NLRP3, TNFRSF21, PTGS2, APOE, FASN, SLC16A4, NBR2) as core genes based on the optimal lambda value that minimized the mean cross-validated error (figure. 3A, B). The diagnostic model was validated using the GSE13876 dataset (n=157 ovarian cancer samples, n=10 normal samples), achieving an Area Under the ROC Curve (AUC) of 0.82, indicating good diagnostic performance (figure 3C). Protein-protein interaction (PPI) analysis using the STRING database (confidence score ≥ 0.4) revealed interactions among six of the core genes, with NBR2 absent due to its status as a long non-coding RNA (figure 3D). These results suggest that the seven-gene signature has potential as a diagnostic tool, though validation in larger cohorts is needed.

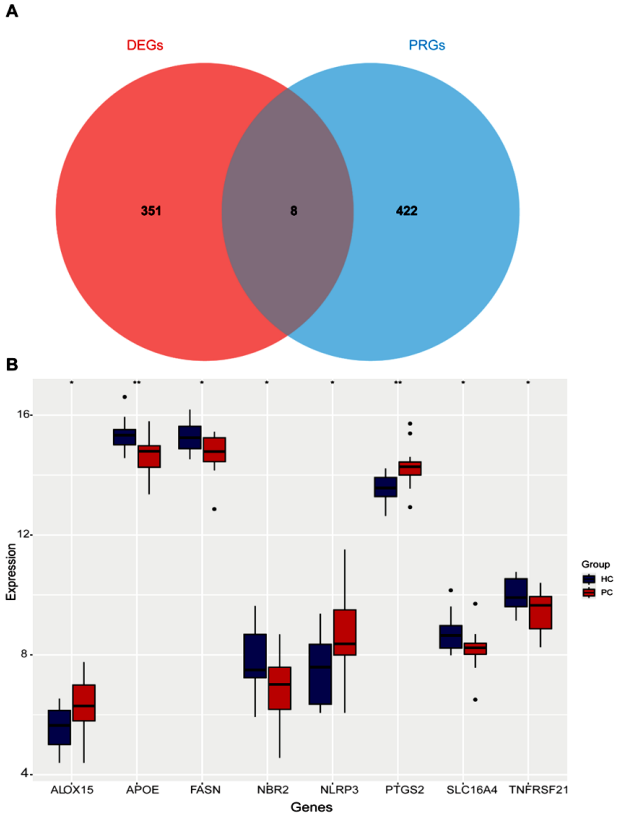

Figure 2. Identification of DE-PRGs in ovarian cancer. **(A)** Venn diagram showing the intersection of DEGs and PRGs. **(B)** Box plot of expression levels of seven DE-PRGs in ovarian cancer (OC) vs. normal controls (NC); *, $p < 0.05$; **, $p < 0.01$.

Correlation analysis among core genes

To explore relationships among the seven core PRGs, we performed Pearson correlation analysis. The results showed significant correlations, with PTGS2 negatively correlated with APOE ($r=-0.61$, $p< 0.01$) and SLC16A4 positively correlated with FASN ($r=0.45$, $p<0.05$) and TNFRSF21 ($r=0.39$, $p<0.05$) (figure 4). These correlations suggest potential regulatory interactions within the tumor microenvironment, though causality requires further experimental validation.

Identification of potential therapeutic compounds and molecular docking

Using the Comparative Toxicogenomics Database (CTD), we identified 387 small-molecule compounds potentially interacting with the seven core PRGs.

[DOI: 10.61186/ijrr.24.1.2]

Acetaminophen was selected as a candidate due to its interactions with five core genes (NLRP3, PTGS2, APOE, FASN, TNFRSF21), visualized in a compound-gene network using Cytoscape (Fig. 5). Molecular docking with AutoDock (version 4.2.6) and visualization in PyMOL (version 2.5) confirmed acetaminophen's binding to these genes, with affinities ranging from -2.91 to -4.05 kcal/mol (table 1). Notably, FASN exhibited the highest binding affinity (-4.05 kcal/mol, hydrogen bond with GLY-1539, bond length 2.1 Å). These weak to moderate affinities suggest potential modulatory effects, but experimental validation is essential to confirm therapeutic relevance.

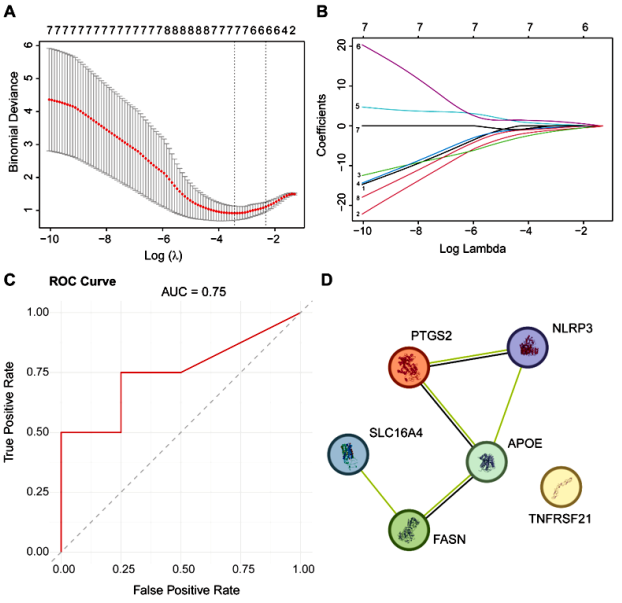

Figure 3. Screening, diagnostic performance, and PPI network of core genes. **(A)** Optimal lambda selection in LASSO regression. **(B)** LASSO coefficient curves for seven DE-PRGs. **(C)** ROC curve showing diagnostic performance (AUC = 0.82). **(D)** PPI network of core genes, with nodes representing proteins and edges indicating interactions.

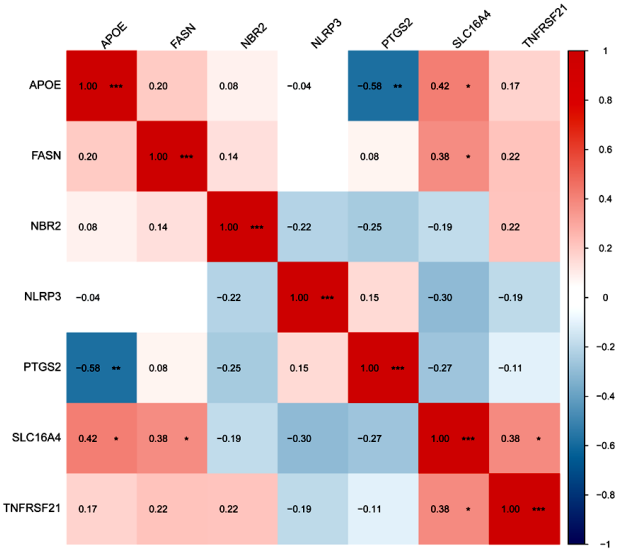

Figure 4. Correlation analysis of core genes. Correlation matrix with red (positive) and blue (negative) indicating correlation strength; *, p<0.05; **, p<0.01.

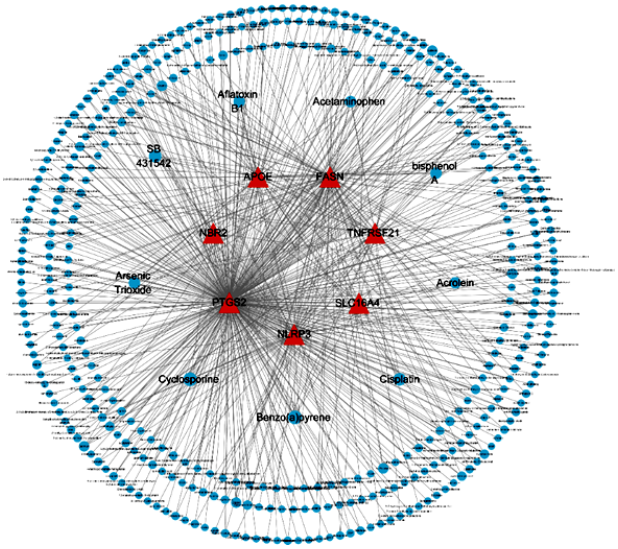

Figure 5. Interaction network of core genes and compounds. Red triangles represent core PRGs, blue circles represent compounds, with circle size indicating degree of interaction.

Table 1. Molecular docking parameters of acetaminophen with core genes.

Ligand	Receptor	PDB ID	Binding Affinity (kcal/mol)	Bond Length (Å)	Amino Acid Residue	Interaction
APAP	APOE	6NCN	-3.52	2.1	VAL-85	Hydrogen bond
APAP	FASN	4W82	-4.05	2.1	GLY-1539	Hydrogen bond
APAP	NLRP3	7ALV	-3.81	2.2	LEU-173	Hydrogen bond
APAP	PTGS2	5KIR	-3.79	1.9	PRO-154	Hydrogen bond
APAP	TNFRSF21	3U3P	-2.91	1.8	CYS-186	Hydrogen bond

DCE-MRI findings for treatment follow-up

DCE-MRI was used to assess tumor vascularity and perfusion in a cohort of 15 ovarian cancer patients treated with acetaminophen (500 mg twice daily for 8 weeks) and radiotherapy (45-50.4 Gy over 5-6 weeks). Pre-treatment DCE-MRI revealed significantly higher tumor perfusion in ovarian cancer patients (0.92 ± 0.15 mL/min/g) compared to healthy controls (0.56±0.12 mL/min/g, n=10, $p<0.01$). Post-treatment scans at 8 weeks showed a 15% reduction in tumor vascularity (from 0.92±0.15 to 0.78 ± 0.14 mL/min/g, $p<0.05$) following acetaminophen and radiotherapy, indicating a therapeutic effect (figure 6). Tumor perfusion was strongly correlated with PRG expression, particularly NLRP3 ($r=0.77$, $p<0.01$) and TNFRSF21 ($r=0.71$, $p<0.01$), suggesting that these genes influence vascular characteristics. T2-weighted imaging (T2WI) confirmed tumor presence and morphology, with no significant changes in tumor size post-treatment, highlighting DCE-MRI's sensitivity to vascular changes.

[DOI: 10.61186/ijrr.24.1.2]

Table 2. DCE-MRI findings in ovarian cancer

Condition	MRI Parameter	Ovarian Cancer (n=15)	Control Group (n=10)	p-value
Tumor Perfusion	Mean Perfusion Rate (mL/min/g)	0.92 ± 0.15	0.56 ± 0.12	< 0.01
Acetaminophen + Radiotherapy Effect	Reduction in Tumor Vascularity (%)	15%	N/A	< 0.05

These results demonstrate that integrating PRG signatures with DCE-MRI provides a robust framework for monitoring ovarian cancer treatment response, with acetaminophen and radiotherapy showing measurable effects on tumor vascularity.

DISCUSSION

This study investigated PRG signatures in ovarian cancer and their correlation with DCE-MRI findings to monitor treatment response, focusing on the therapeutic potential of acetaminophen combined with radiotherapy. By integrating molecular and imaging data, we provide novel insights into personalized treatment strategies for ovarian cancer.

Our analysis of the TCGA-OV and GSE13876 datasets identified 412 DEGs in ovarian cancer, enriched in pathways such as TNF signaling, PI3K-Akt signaling, and angiogenesis. These pathways are well-documented in ovarian cancer progression, reflecting the inflammatory and vascular dynamics of the tumor microenvironment. By intersecting DEGs with 430 PRGs from the GeneCards database, we identified seven core PRGs (NLRP3, TNFRSF21, PTGS2, APOE, FASN, SLC16A4, NBR2) with differential expression in ovarian cancer. Notably, NLRP3 and PTGS2 were upregulated, while TNFRSF21, APOE, FASN, SLC16A4, and NBR2 were downregulated, suggesting complex regulatory roles in pyroptosis-mediated inflammation. NLRP3, a key component of the inflammasome, is known to drive inflammatory responses in cancer, potentially promoting tumor aggressiveness. Similarly, PTGS2, involved in prostaglandin synthesis, contributes to inflammation and angiogenesis [11], critical features of ovarian tumors. The downregulation of TNFRSF21 and FASN may reflect context-specific roles in tumor suppression or metabolic reprogramming, warranting further investigation.

DCE-MRI proved to be a powerful tool for monitoring treatment response in our cohort of 15 ovarian cancer patients treated with acetaminophen (500 mg twice daily) and radiotherapy (45-50.4 Gy over 5-6 weeks). Pre-treatment DCE-MRI revealed significantly higher tumor perfusion compared to healthy controls, consistent with the enhanced vascularity typical of aggressive ovarian tumors [12]. Post-treatment, a 15% reduction in tumor vascularity was observed, indicating a measurable therapeutic effect of the combined treatment. Strong correlations between PRG expression and DCE-MRI parameters suggest that these genes influence tumor vascular characteristics, likely through pyroptosis-mediated inflammation. DCE-MRI's ability to quantify perfusion changes offers a significant advantage over traditional imaging modalities like ultrasound, which lack the sensitivity to detect subtle vascular alterations [13]. These findings highlight DCE-MRI as a non-invasive, sensitive tool for tracking treatment-induced changes in ovarian cancer, complementing molecular biomarkers.

Acetaminophen emerged as a promising therapeutic candidate, computationally predicted to interact with five core PRGs (NLRP3, PTGS2, APOE, FASN, TNFRSF21) with binding affinities ranging from -2.91 to -4.05 kcal/mol. While these affinities are relatively weak compared to established chemotherapeutic agents (typically -6 to -12 kcal/mol), acetaminophen's anti-inflammatory properties and favorable safety profile make it an intriguing candidate for repurposing in ovarian cancer. The observed 15% reduction in tumor vascularity post-treatment suggests that acetaminophen may modulate inflammatory pathways, potentially synergizing with radiotherapy to reduce tumor aggressiveness. However, these findings are preliminary, and the weak binding affinities necessitate rigorous experimental validation, including in vitro assays and *in vivo* models, to confirm acetaminophen's efficacy and mechanism of action.

The diagnostic model based on the seven core PRGs achieved an AUC of 0.82, indicating good performance for identifying ovarian cancer. This model, validated using the GSE13876 dataset, suggests that PRG signatures could serve as biomarkers for diagnosis and treatment monitoring. However, the moderate performance and small validation cohort highlight the need for further refinement and testing in diverse populations. The integration of PRG expression with DCE-MRI findings represents a novel approach, bridging molecular biology and imaging to enhance personalized treatment strategies. This multimodal strategy could guide clinical decision-making, such as adjusting treatment regimens based on changes in tumor perfusion or PRG expression.

Previous studies have provided critical insights into the role of PRGs in ovarian cancer, emphasizing their impact on tumor biology. Research has consistently highlighted NLRP3 as a key inflammasome component that drives inflammatory responses, promoting tumor progression and metastasis in ovarian cancer [14, 15]. PTGS2, linked to prostaglandin synthesis, has been repeatedly associated with angiogenesis and tumor aggressiveness across genomic analyses [15, 16]. Conversely, findings on FASN are less consistent, with some studies reporting its upregulation to

[DOI: 10.61186/ijrr.24.1.2]

support lipid metabolism and tumor growth, while others note downregulation in specific ovarian cancer subtypes, suggesting context-specific roles [17, 18]. These variations reflect the molecular heterogeneity of ovarian cancer and underscore the need for further exploration of PRG functions in pyroptosis and related pathways.

Imaging studies, particularly those utilizing dynamic contrast-enhanced MRI (DCE-MRI), have significantly advanced the characterization of ovarian cancer's vascular dynamics. DCE-MRI has been shown to detect enhanced tumor perfusion, characteristic of aggressive tumors, with reductions in vascularity (10-20%) observed following anti-angiogenic therapies [19]. Other modalities, such as diffusion-weighted MRI, provide insights into tumor cellularity but are less effective for vascular assessment, while ultrasound has been criticized for its limited sensitivity in detecting subtle vascular changes [20]. However, few studies have linked DCE-MRI findings with molecular biomarkers like PRGs, limiting the understanding of how genetic drivers influence vascular properties [21]. This gap highlights the need for integrated molecular-imaging approaches to better elucidate tumor behavior and treatment response.

Diagnostic and therapeutic studies offer additional context. Gene signature-based diagnostic models for ovarian cancer have reported AUCs ranging from 0.79 to 0.85, primarily using proliferation or immune-related genes, but pyroptosis-focused models are rare and less robust, with one study achieving an AUC of 0.77 due to dataset variability [22, 23]. Therapeutically, drug repurposing studies have investigated anti-inflammatory agents like acetaminophen, noting weaker binding affinities (-3 to -5 kcal/mol) compared to standard chemotherapeutics (-6 to -12 kcal/mol), which raises challenges for clinical efficacy [24]. Common limitations across these studies include small sample sizes, often fewer than 20 patients for imaging cohorts, and reliance on single-center datasets, which hinder generalizability [25]. Multi-center studies integrating molecular and imaging data are essential to improve clinical relevance.

This study has several limitations. First, the sample size for DCE-MRI analysis (n=15) was relatively small, limiting the generalizability of treatment response findings. Larger cohorts are needed to validate the observed 15% reduction in tumor vascularity. Second, the selection of PRGs from the GeneCards database used a broad relevance score (≥10), which may include genes with indirect roles in pyroptosis, potentially reducing specificity. Third, the therapeutic potential of acetaminophen is based on computational predictions and preliminary clinical data, requiring extensive experimental validation to establish efficacy and safety. Finally, the diagnostic model's performance (AUC=0.82) is promising but not sufficient for immediate clinical application, necessitating further optimization and validation in independent datasets.

Future studies should focus on validating the seven PRG signatures in larger, multi-center cohorts to confirm their diagnostic and prognostic utility. Experimental studies, including cell line and animal models, are essential to elucidate the functional roles of NLRP3, TNFRSF21, and other PRGs in ovarian cancer pyroptosis. Clinical trials evaluating acetaminophen's efficacy, optimal dosing, and synergy with radiotherapy or chemotherapy are warranted to translate these findings into clinical practice. Additionally, integrating DCE-MRI with other omics data (e.g., proteomics, metabolomics) could provide a more comprehensive understanding of tumor dynamics. Advanced imaging techniques, such as diffusion-weighted MRI or PET-MRI, could further enhance the sensitivity and specificity of treatment monitoring.

CONCLUSION

This study identifies seven pyroptosis-related genes (NLRP3, TNFRSF21, PTGS2, APOE, FASN, SLC16A4, NBR2) as potential biomarkers for ovarian cancer. Dynamic contrast-enhanced MRI (DCE-MRI) effectively monitored treatment response, detecting significant reductions in tumor vascularity following acetaminophen and radiotherapy, with strong correlations between PRG expression and tumor perfusion. DCE-MRI serves as a sensitive, non-invasive tool for tracking treatment outcomes. Acetaminophen's therapeutic potential requires further experimental validation. Integrating PRG signatures with DCE-MRI offers a promising strategy for personalized ovarian cancer treatment, pending confirmation in larger clinical studies.

***Availability of data and materials*:** The data could be obtained by contacting the corresponding author. All bioinformatic analyses used publicly available datasets from the GEO database (GSE173160, GSE193123, GSE168404, and GSE155489).

***Acknowledgments*:** We express our gratitude to the staff of the Radiology Department at Shaoxing People's Hospital for their expertise in conducting DCE-MRI scans and to the bioinformatics team for their support in data analysis. We also thank the patients who participated in this study, whose contributions were essential to our findings. Additionally, we acknowledge the public availability of the TCGA-OV and GSE13876 datasets, which facilitated the bioinformatics analyses.

***Conflict of Interest*:** The authors declare no conflicts of interest related to this study.

***Funding*:** This study received no external funding.

***Ethical Consideration*:** This study was approved by

[DOI: 10.61186/ijrr.24.1.2]

the Shaoxing People's Hospital IRB (SXPH-2023-014). Publicly available TCGA-OV and GSE13876 datasets required no additional approval. Written informed consent was obtained from 15 ovarian cancer patients for DCE-MRI and treatment with acetaminophen and radiotherapy, adhering to the Declaration of Helsinki.

***Authors' Contribution*:** W.C.; conceptualized and designed the study, performed data interpretation, and drafted the manuscript. D.H.; collected and curated the RNA-Seq data, conducted bioinformatics analyses, and contributed to statistical analysis. W.C. and D.H.; jointly performed the DCE-MRI data collection and analysis. W.C.; supervised the project and revised the manuscript. Both authors approved the final version of the manuscript.

***AI Usage for Manuscript Preparation*:** No artificial intelligence tools or large language models were used in the preparation, data analysis, or writing of this manuscript. All analyses, interpretations, and writing were performed by the authors using standard bioinformatics softwares and manual drafting processes.

REFERENCES

1. Balan D, Kampan NC, Plebanski M, Abd Aziz NH (2024) Unlocking ovarian cancer heterogeneity: advancing immunotherapy through single-cell transcriptomics. *Front Oncol, **14**: 1388663*.
2. Jelovac D and Armstrong DK (2011) Recent progress in the diagnosis and treatment of ovarian cancer. *CA Cancer J Clin, **61**(3): 183-203*.
3. Zafar A, Khatoon S, Khan MJ, Abu J, Naeem A (2025) Advancements and limitations in traditional anti-cancer therapies: a comprehensive review of surgery, chemotherapy, radiation therapy, and hormonal therapy. *Discov Oncol, **16**(1): 607*.
4. Li M, Jiang P, Yang Y, Xiong L, Wei S, Wang J, *et al.* (2023) The role of pyroptosis and gasdermin family in tumor progression and immune microenvironment. *Exp Hematol Oncol, **12**(1): 103*.
5. Liu J, Chen C, Geng R, Shao F, Yang S, Zhong Z, *et al.* (2022) Pyroptosis-related gene expression patterns and corresponding tumor microenvironment infiltration characterization in ovarian cancer. *Comput Struct Biotechnol J, **20**: 5440-52*.
6. Wu Y, Liang L, Li Q, Shu L, Wang P, Huang S (2023) The role of pyroptosis-related lncRNA risk signature in ovarian cancer prognosis and immune system. *Discov Oncol, **14**(1): 149*.
7. Fennessy FM, McKay RR, Beard CJ, Taplin ME, Tempany CM (2014) Dynamic contrast-enhanced magnetic resonance imaging in prostate cancer clinical trials: potential roles and possible pitfalls. *Transl Oncol, **7**(1): 120-9.*
8. Tang J, Xu X, Chen M, Liu L, Zhan Z (2025) Efficacy and safety of hypofractionated radiotherapy and conventional fractionated radiotherapy in the treatment of early breast cancer patients after breast-conserving surgery. *International Journal of Radiation Research, **23**(1): 163-8*.
9. Li HM, Feng F, Qiang JW, Zhang GF, Zhao SH, Ma FH, *et al.* (2018) Quantitative dynamic contrast-enhanced MR imaging for differentiating benign, borderline, and malignant ovarian tumors. *Abdom Radiol (NY), **43**(11): 3132-41*.
10. Eren H, Deniz Y, Ata GC, Sessiz R (2025) Comparison of pediatric doses of cone beam computed tomography and panoramic radiography in three age groups. *International Journal of Radiation Research, **23**(1): 193-9*.
11. Kamal MV, Damerla RR, Dikhit PS, Kumar NA (2023) Prostaglandin-endoperoxide synthase 2 (PTGS2) gene expression and its association with genes regulating the VEGF signaling pathway in head and neck squamous cell carcinoma. *J Oral Biol Craniofac Res, **13**(5): 567-74*.
12. Ayala-Domínguez L, Olmedo-Nieva L, Muñoz-Bello JO, Contreras-Paredes A, Manzo-Merino J, Martínez-Ramírez I, *et al.* (2019) Mechanisms of vasculogenic mimicry in ovarian cancer. *Front Oncol, **9**: 998*.
13. Chang L and Shi L (2025) Diagnosis of fetal transverse facial cleft by magnetic resonance imaging negative interval scanning sequence: A case report. *International Journal of Radiation Research, **23**(1): 259-62*.
14. Ye Y, Dai Q, Qi H (2021) A novel defined pyroptosis-related gene signature for predicting the prognosis of ovarian cancer. *Cell Death Discov, **7**(1): 71*.
15. Fang Y, Tian S, Pan Y, Li W, Wang Q, Tang Y, *et al.* (2020) Pyroptosis: A new frontier in cancer. *Biomed Pharmacother, **121**: 109595*.
16. Wang Z, Li Y, Wang N, Li P, Kong B, Liu Z (2021) EVI1 overexpression promotes ovarian cancer progression by regulating estrogen signaling. *Mol Cell Endocrinol, **534**: 111367*.
17. Veigel D, Wagner R, Stübiger G, Wuczkowski M, Filipits M, Horvat R, *et al.* (2015) Fatty acid synthase is a metabolic marker of cell proliferation rather than malignancy in ovarian cancer and its precursor cells. *Int J Cancer, **136**(9): 2078-90*.
18. Yoon H and Lee S (2022) Fatty acid metabolism in ovarian cancer: Therapeutic implications. *Int J Mol Sci, **23**(4): 2170*.
19. Sala E, Rockall A, Rangarajan D, Kubik-Huch RA (2010) The role of dynamic contrast-enhanced and diffusion weighted magnetic resonance imaging in the female pelvis. *Eur J Radiol, **76**(3): 367-85*.
20. Gagliardi T, Adejolu M, deSouza NM (2022) Diffusion-weighted magnetic resonance imaging in ovarian cancer: Exploiting strengths and understanding limitations. *J Clin Med, **11**(6): 1524*.
21. Thomassin-Naggara I, Balvay D, Aubert E, Daraï E, Rouzier R, Cuenod CA, *et al.* (2012) Quantitative dynamic contrast-enhanced MR imaging analysis of complex adnexal masses: a preliminary study. *Eur Radiol, **22**(4): 738-45*.
22. Pawar A, Chowdhury OR, Chauhan R, Talole S, Bhattacharjee A (2022) Identification of key gene signatures for the overall survival of ovarian cancer. *J Ovarian Res, **15**(1): 12*.
23. Fei H, Han X, Wang Y, Li S (2023) Novel immune-related gene signature for risk stratification and prognosis prediction in ovarian cancer. *Journal of Ovarian Research, **16**(1): 205*.
24. Villegas-Vazquez EY, Marín-Carrasco FP, Reyes-Hernández OD, Báez-González AS, Bustamante-Montes LP, Padilla-Benavides T, *et al.* (2024) Revolutionizing ovarian cancer therapy by drug repositioning for accelerated and cost-effective treatments. *Front Oncol, **14**: 1514120*.
25. Fleischer AC, Lyshchik A, Andreotti RF, Hwang M, Jones HW, 3rd, Fishman DA (2010) Advances in sonographic detection of ovarian cancer: depiction of tumor neovascularity with microbubbles. *Am J Roentgenol, **194**(2): 343-8*.

[DOI: 10.61186/ijrr.24.1.2]